

# Hydrogen release from aqueous based LOHCs: The role of water in the potassium formate/bicarbonate cycle

*Mark E. Bowden\*<sup>1</sup>, Denzel Megafu,<sup>1</sup> Tom Autrey<sup>1</sup>, Karsten Müller\*<sup>2</sup>*

<sup>1</sup> Pacific Northwest National Laboratory, 902 Battelle Boulevard, Richland, WA 99352, United States

<sup>2</sup> University of Rostock, Institute of Technical Thermodynamics, Albert--Einstein-Str. 2, 18059 Rostock, Germany

## **Abstract**

In this study, we evaluate the chemical and physical properties governing the potential efficiency of an aqueous potassium formate/bicarbonate cycle for hydrogen storage. Using thermodynamic parameters, we predict the conversion of formate to bicarbonate across varying temperatures and pressures, revealing that hydrogen release is relatively insensitive to temperature but highly dependent on pressure. We calculate the solubility limits of bicarbonate salts influenced by the common ion effect to predict conversion ranges that prevent precipitation of potassium bicarbonate in a reactor. Furthermore, the energy efficiency of hydrogen release is assessed based on the heating requirements of the aqueous solutions. This analysis balances the solubility limits of bicarbonate, the heat capacity of aqueous formate solutions, and conversion based on thermodynamic equilibria. Taking these factors into consideration we suggest reaction conditions that could be utilized in a systems analysis to calculate the levelized cost of storage using the bicarbonate/formate cycle at commercial scales.

**Keywords:** hydrogen storage, liquid hydrogen carrier, thermodynamics, common ion effect

## 1. Introduction

Liquid organic hydrogen carriers (LOHCs) are carbon-based molecules that are used to store and transport hydrogen in liquid form at ambient temperatures and pressure. [1-5] Candidates for LOHCs consist of a broad range of molecules such as formic acid [6], aqueous formate salts, [7] alcohols [8, 9], aromatic [4, 5, 10], and heterocyclic compounds [11-13] providing a theoretical volumetric hydrogen density ranging between ca. 20-60 kg H<sub>2</sub>/m<sup>3</sup>. Reaction thermodynamics is a defining property for the release of hydrogen and regeneration of the depleted carrier that impacts both conversion and energy efficiency. Formic acid is unusual in that release of hydrogen is exergonic,  $\Delta^rG$  ca. -31 kJ mol<sub>H<sub>2</sub></sub><sup>-1</sup> ( $\Delta^rH$  ca. +30 kJ/mol<sub>H<sub>2</sub></sub><sup>-1</sup>) [14, 15], whereas release of hydrogen is comparatively unfavorable for other LOHCs, e.g. MCH and H18-DBT,  $\Delta^rG$  ca. +33 kJ mol<sub>H<sub>2</sub></sub><sup>-1</sup> ( $\Delta^rH$  ca. +68 kJ mol<sub>H<sub>2</sub></sub><sup>-1</sup>) [10, 16]. Aqueous formate salts are particularly interesting due to favorable thermodynamics,  $\Delta^rG$  ca. 1 kJ mol<sub>H<sub>2</sub></sub><sup>-1</sup> ( $\Delta^rH$  ca. 20 kJ mol<sub>H<sub>2</sub></sub><sup>-1</sup>) [17], which allows hydrogen uptake and release at moderate temperatures and pressures. In addition to providing a liquid phase as a solvent, water provides half of the hydrogen during hydrogen release [18] in a manner comparable to aqueous sodium borohydride. In both systems the products formed from hydrogen release, bicarbonate and metaborate, are less soluble than the corresponding formate and borohydride, and this solubility needs to be considered in a practical system [19-21]. On the other hand, unlike aq. NaBH<sub>4</sub>, the hydrolysis of a formate salt to release H<sub>2</sub> is reversible and can serve as a round-trip hydrogen carrier [22-25]. Potassium formate is an attractive option based on large scale availability and safety perspectives. In previous work we defined the limits of using formate salts to store, transport and release hydrogen based on their solubility and that of the corresponding bicarbonates at ambient temperatures [26]. Potassium formate is very soluble in water, up to 75 wt.% (14 M), and sold commercially as a road deicer. The theoretical hydrogen capacity, ca. 28 kg H<sub>2</sub>/m<sup>3</sup>, is equivalent to the density of compressed H<sub>2</sub> at 400 bar. However, potassium bicarbonate is less soluble, ca. 3 M at room temperature, requiring dilution of the formate salt to maintain a single phase and avoid precipitation. While the precipitation of KHCO<sub>3</sub> does not appear to stop hydrogen production in a batch reactor, it would be challenging to accommodate in a flow reactor that would be required for large scale hydrogen storage applications. [27]

Our aim in this paper is to determine the effect that water has on the capacity and efficiency of hydrogen release taking into consideration (i) the conversion limited by equilibrium (ii) the solubility limit of mixtures of KHCO<sub>2</sub> and KHCO<sub>3</sub> due to a common ion effect and (iii) the heat capacity of aqueous formate solutions. Higher concentrations of formate have lower heat

capacities and will increase efficiency, but must be balanced with the need to maintain solubility. Solubility data is available for the individual salts but there is little solubility data for mixtures. We calculate the solubilities of mixed potassium formate/bicarbonate systems using the solubility product incorporating the common ion effect. With this insight combined with thermodynamic equilibrium, we determine conditions to provide high energy efficiency while retaining solubility and storage capacity. This information is helpful to advance hydrogen storage using aqueous potassium formate beyond the lab bench using methods such as systems and techno-economic analyses.

## 2. Methods

Thermodynamic equilibria were calculated using the Gibbs Energy Minimizer of HSC Chemistry, a thermodynamic software package available from Metso Finland Oy. The software finds the lowest free energy composition of selected chemical species given a starting composition and conditions of temperature and pressure or volume, using a database of thermodynamic values compiled by the vendor.

Energy efficiency was calculated using the energy input required to release hydrogen and the lower heating value of H<sub>2</sub>. The energy input is the sum of the reaction enthalpy (20 kJ/mol<sub>H<sub>2</sub></sub>), the heat of evaporation for the share of the water that is transferred to the gas phase, and the energy required to heat the solution. The latter was calculated as  $c_p \cdot \Delta T$  where  $c_p$  is the average of the heat capacities of the formate solutions at 20 °C and the reaction temperature and  $\Delta T$  is the difference between the reaction temperature and 20 °C. Heat capacities were calculated using the polynomials published by Wen et al. [28].

Solubilities at room temperature were determined by mixing concentrated solutions of potassium formate and bicarbonate and gradually adding DI water until no solids could be observed upon rapid agitation. The masses of all components were recorded and used to calculate the saturation composition.

## 3. Results and Discussion

### 3.1 Thermodynamic equilibrium conversion.

Thermodynamic calculations of the equilibria between aqueous formate, bicarbonate, gaseous H<sub>2</sub>, and other products can provide insights into the reaction conditions that favor H<sub>2</sub> release and uptake. Figure 1a shows the calculated thermodynamic maximum conversion (fraction of

formate reacted to produce H<sub>2</sub>) as a function of concentration and temperature for a total pressure of 1 bar. The highest conversions are observed at high temperature and concentration, and inspection of the data showed there are two factors responsible:

1. High partial pressures of water at high temperature, which lowers the partial pressure of H<sub>2</sub> through dilution since the total pressure is fixed at 1 bar.
2. Precipitation of KHCO<sub>3</sub> at high K<sup>+</sup> concentrations.

Both of these factors increase conversion through Le Chatelier's principle by lowering the activity of products in the overall reaction:



Prediction of solubility using general thermodynamic data is often inaccurate because the values for different species are obtained from disparate studies and the differences in  $\Delta G$  between solid and dissolved species may not be large. The calculated  $\Delta G^\circ$  for solid KHCO<sub>3</sub> at 25 °C is -867.1 kJ/mol, and the sum of K<sup>+</sup>(aq.) and HCO<sub>3</sub><sup>-</sup>(aq.) is -869.3 kJ/mol. The equilibrium depends on the difference between these values and is only 0.26 % of either value, meaning that a high accuracy is needed for predicting solubility. Our calculations suggest that this accuracy is lacking in HSC Chemistry, which predicts much higher KHCO<sub>3</sub> solubility at low temperature than observed experimentally, and an unintuitive decrease in solubility with increasing temperature (Figure S2). This results in significant quantities of solid KHCO<sub>3</sub> and consequently large conversions being calculated for the upper right region of Figure 1a. Large conversions are also calculated at high temperatures and low K<sup>+</sup> concentrations, but this is a consequence of the high vapor pressure of water in this case. It should be noted that the accuracy of HSC Chemistry to reproduce experimental equilibria is mostly confined to solid phases in these systems, and that good agreement is obtained with literature experimental solution equilibria (Fig. S3).

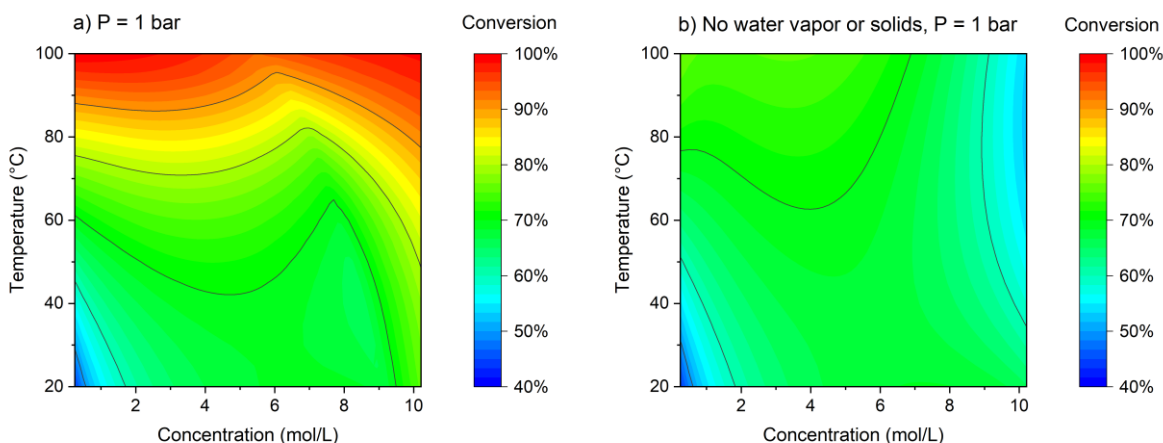


**Figure 1.** a) Calculated equilibrium conversion of potassium formate to hydrogen as a function of temperature and  $K^+$  concentration, at a total pressure of 1 bar. b) Calculated conversion without gaseous  $H_2O$  and solid  $KHCO_3$  as potential products to illustrate the effect of these species on the equilibrium. The solid contour lines are drawn at conversions which are integer multiples of 10%.

The influence of  $H_2$  dilution by water vapor and precipitation of  $KHCO_3$  can be seen by comparing Figure 1a with Figure 1b, where  $H_2O(gas)$  and  $KHCO_3(s)$  have been removed hypothetically as possible equilibrium products. Without dilution and precipitation, the calculated conversion is approximately 70% for all temperatures and concentrations. Dilution by water vapor is larger than 80% at temperatures near 100 °C and concentrations below 3M (Figure S4). The dilution is still significant at 80°C, where the calculated partial pressure of water vapor ranges between 0.31 atm (10 M) and 0.46 atm (1 M), reducing the partial pressure of  $H_2$  to a maximum of 0.54 – 0.69 atm. Utilizing water vapor to lower  $H_2$  partial pressure is an unexpected way of increasing conversion, although at the expense of additional energy demand for the latent heat of vaporization. Heat recovery from the reactor outlet could be used to offset this demand and improve efficiency. The heat that could be recovered from the hot product stream consists of two contributions: sensible heat for cooling the gas and latent heat for condensing the vapor. While the amount of the first is more or less proportional to the decrease in temperature, latent heat is recovered within the temperature range of condensation. An analysis of latent heat recovery is shown in Section 3.5 for conditions chosen to balance efficiency and storage capacity.

The equilibrium conversion is much more sensitive to the partial pressure of  $H_2$  than to temperature within the relevant parameter range, as Figure 2 illustrates for 5 M potassium formate. For example, heating the solution at 1 bar from 40 to 80 °C increases the equilibrium

conversion for hydrogen release from 70% to 84%. However, keeping the solution at 80 °C and increasing the pressure from 1 bar to 5 bar decreases the fraction of H<sub>2</sub> released from 84% to 23%. This shows the large potential for operation at low pressure for improving reaction thermodynamics of dehydrogenation. For example, greater conversion of formate to bicarbonate and H<sub>2</sub> can be obtained at 40 °C and 1 bar than at 80 °C and 5 bar. Higher temperatures may be required to obtain the required rates, but the reactor should be operated at lower pressures to allow sufficient conversion, at least at the price of a low space-time-yield. Interestingly, the equilibrium conversion is not greatly affected by concentration, with only minor differences evident for the calculated conversions at 1 and 10 M potassium formate (Figure S5).

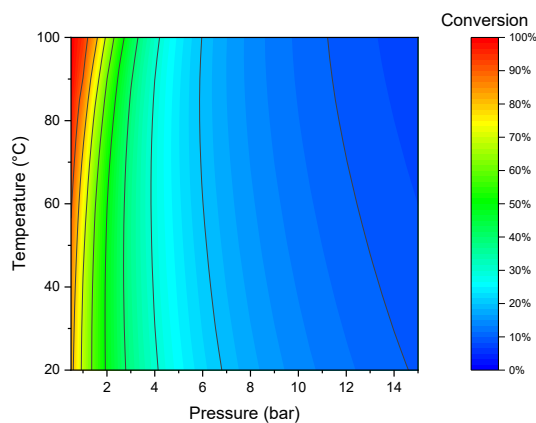


**Figure 2.** Contour plot showing the equilibrium conversion (fraction of hydrogen released) of 5 M aqueous potassium formate solution as a function of temperature and pressure. The solid contour lines are drawn at conversions which are integer multiples of 10%.

The equilibria in Figures 1 and 2 are independent from the starting composition and therefore can be used to find favored reaction conditions for hydrogenation of bicarbonate to formate. Conversion in these figures is presented for the release of hydrogen, but the degree of hydrogenation can be determined by simply subtracting the conversion from 100%. Figure 2 shows that thermodynamically, relatively low H<sub>2</sub> pressures are sufficient for high degrees of hydrogenation. For example, heating a 5 M bicarbonate solution at 60 °C under 10 bar H<sub>2</sub> allows for a maximum conversion back to formate of 88%.

### 3.2 Common ion effect, solubility limits of potassium formate/bicarbonate mixtures

The solubility of pure potassium formate and bicarbonate salts as a function of temperature are documented in the literature and are shown in Figure S6. However, in mixtures of these salts, their solubility does not follow a simple linear relationship due to the common ion effect. For example,  $\text{KHCO}_3$  solution is completely soluble at 3 M at room temperature but will precipitate solids when mixed with  $\text{KHCO}_2$  if the ionic product of  $\text{K}^+$  and  $\text{HCO}_3^-$  exceeds the solubility product; i.e.  $[\text{K}^+][\text{HCO}_3^-] > K_{sp}$ . Precipitation of solids is an issue if it leads to clogged reactors or pumps, and settling of solids in storage tanks will add an additional operation unit making full hydrogenation/dehydrogenation cycles more challenging.

Precipitation can be avoided by limiting either the overall  $[\text{K}^+]$  concentration, the degree of conversion, or a combination of both. To investigate this, the solubility of mixed formate/bicarbonate solutions was calculated as a function of temperature. Since  $\text{KHCO}_3$  is less soluble than  $\text{KHCO}_2$  (Figure S6), only the solubility product of  $\text{KHCO}_3$  is considered.  $K_{sp}$ , in  $\text{mol}^2(\text{kg water})^{-2}$ , was calculated from the temperature dependent solubility shown in the Supplementary Information. A linear fit to these data agreed with the experimental values to within  $\pm 0.7\%$  for 21 of the 22 data points, and was extrapolated beyond the 60 °C data limit for subsequent calculations. Solubilities are frequently linear over a large temperature range, for example the data shown for potassium formate is linear between 10 and 80 °C, and therefore the fit and its extrapolation have little impact on the reliability of our model. Solubility products are typically calculated in units of solubility rather than activity. Although this may limit their accuracy in multi-component systems, it is sufficient to demonstrate the principles and meet the objective of the present study of finding reaction conditions favorable for formate dehydrogenation.

Figure 3 shows the calculated conversion limit before  $\text{KHCO}_3$  precipitation at various temperatures as a function of initial  $\text{KHCO}_2$  concentration. This was calculated from  $K_{sp}$  using the approach described in the SI with the x-axis converted to molarity for convenience. Experimental mixtures of  $\text{KHCO}_3/\text{KHCO}_2$  solutions (expressed as conversion) which did not show any solids at room temperature are also plotted as circles in Figure 3 and show the same trend of conversion with concentration as the calculated lines. Weiner et al. [29] presented a similar plot of formate vs. bicarbonate concentrations at 35 °C which is consistent with these calculations. Since water is a reactant for hydrogen release (eq. 1), the solutions will become more concentrated with increasing conversion from the loss of water. This is not widely discussed in the literature, but has an impact on solubility as shown by the dashed lines in Figure

3. For a given temperature and concentration, the loss of water reduces the conversion that can be reached before precipitation. The importance of ignoring this effect is greater for higher conversions and more concentrated solutions.

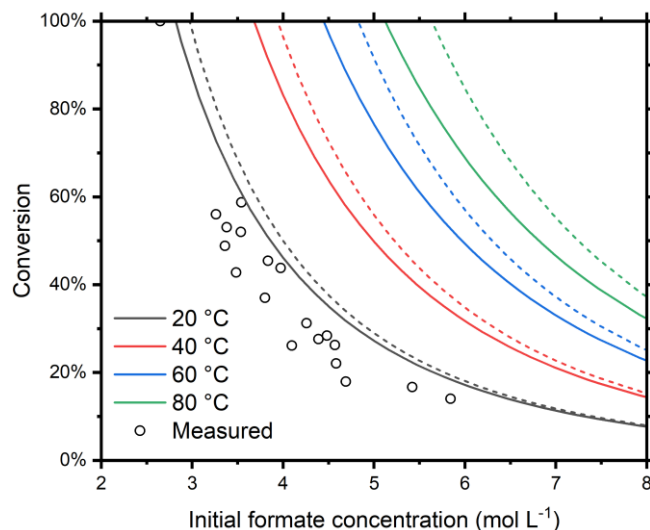


**Figure 3.** Maximum conversion during hydrogen release before precipitation of  $\text{KHCO}_3$  calculated from its  $K_{sp}$ . The solid lines include the loss of water for the hydrogen release reaction; the dashed lines ignore this. The points show measured compositions at room temperature which showed no sign of precipitation.

This analysis of solubility shows that, contrary to intuition, a more concentrated solution may not produce more  $\text{H}_2$  once precipitation is taken into account. For example, an 8 M solution at 80 °C is limited to 32 % conversion, yielding ca. 5.2 g  $\text{H}_2/\text{L}$ . But a 6 M formate solution can attain 69 % conversion before precipitation at the same temperature and release ca. 8.2 g  $\text{H}_2/\text{L}$ . The maximum quantity of  $\text{H}_2$  attainable from  $\text{KHCO}_2$  solutions based on these solubility limits is plotted in Figure 4. The straight line portion toward the upper left represents 100% conversion, which may not be attainable because of the thermodynamic constraints discussed above. It is interesting how steeply the attainable  $\text{H}_2$  capacity drops with increasing concentration and shows that there is an optimum concentration at each temperature which will provide the greatest quantity of  $\text{H}_2$ .

It should be recognized that these solubility calculations are based on somewhat ideal conditions and that the dynamic environment in a continuous flow reactor may present further complications that affect precipitation. It may be necessary to employ engineering solutions

such as actively heated tubing between the reactor and downstream components and/or injection of additional water near the reactor outlet to control precipitation in a practical implementation of this process.

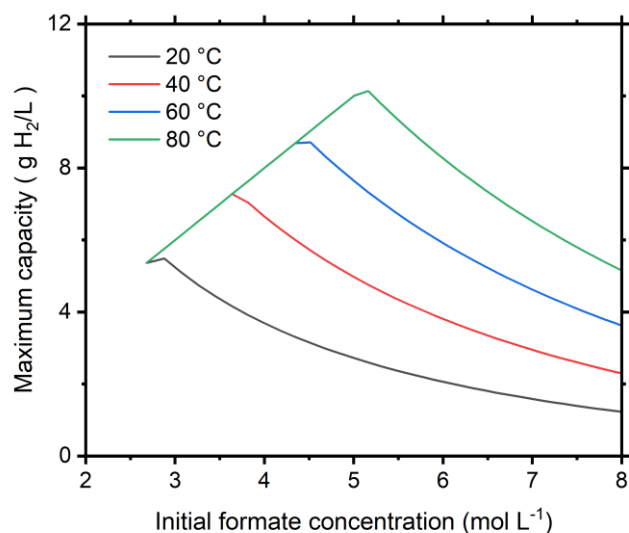


**Figure 4.** Maximum quantity of H<sub>2</sub> that can be released from KHCO<sub>2</sub> solutions based solely on the solubility limits of KHCO<sub>3</sub> calculated in Figure 3.

### 3.3 Energy Efficiency

Water content plays a central role from an energy technological perspective. A crucial factor in this regard is energy efficiency, calculated in this study as:

$$\eta = \frac{E_{out} - E_{in}}{E_{out}}$$

$E_{out}$  is the lower heating value of hydrogen (241.9 kJ/mol), and  $E_{in}$  is the energy needed to release that quantity of hydrogen through the supply of heat. This heat demand for release of hydrogen is more than the 20 kJ/mol reaction enthalpy; additional heat must be supplied to bring the aqueous solution of formate to the reaction temperature. Recuperation of a share of this heat via internal heat integration could reduce this heat demand. Nevertheless, there will be a significant heat demand for preheating in any scenario. Given the large heat capacity of water, the energy needed will be greater for more dilute formate solutions, and become even more pronounced as the temperature for hydrogen release is increased. This is illustrated in Figure 5,

which shows the energy efficiency as a function of formate concentration at various temperatures. At high formate concentration, the sensitivity of efficiency on concentration is limited and concentrations greater than 3 M have efficiencies  $> \sim 60\%$ . As the formate concentration falls below about 3 M, sensitivity becomes more pronounced and the efficiency becomes increasingly lower with dilution. Even negative efficiencies are possible (i.e. energy demand for hydrogen release exceeds the lower heating value of the hydrogen released) for concentrations less than ca. 1 M. As a consequence, high concentrations of formate are favored to achieve higher energy efficiencies.

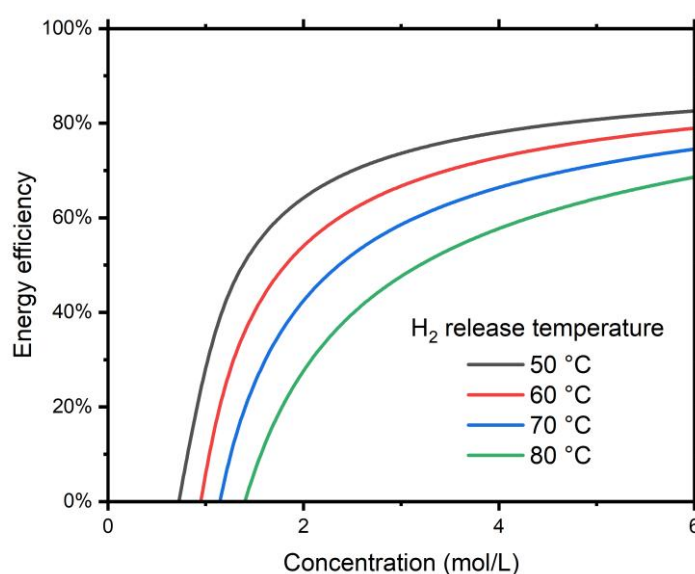


**Figure 5:** Efficiency of hydrogen release in an aqueous bicarbonate/formate system as a function of concentration at different temperatures with no internal heat integration. Full conversion of formate to hydrogen is assumed.

The energy efficiencies plotted in Figure 5 assume full conversion of formate to hydrogen. However, we have shown earlier how reaction thermodynamics and bicarbonate solubility impose theoretical and practical limits on conversion. Lower efficiencies are calculated when these are taken into account. This is shown in Figure 6 for the minimum of either the thermodynamic conversion or the conversion before bicarbonate precipitation at 20 °C (Figure 6a) or the reaction temperature (Figure 6b). In both cases, the efficiencies decrease with increasing reaction temperature for the reasons discussed above. However, they show an optimum concentration depending on the temperature considered.  $\sim 3\text{M}$  formate solutions

provide the highest efficiency when no precipitation is allowed to occur at 20 °C or lower. At higher concentrations, the common ion effect limits conversion (and therefore  $E_{out}$ ) to an extent that overwhelms the efficiency benefits from heating less water. At the extreme conditions of > 6 M formate and reaction > 75 °C the efficiency even becomes negative. Higher efficiencies with more concentrated solutions are achievable if the avoidance of precipitation is confined to the reactor temperature (Figure 6b). Higher reactor temperatures allow increased conversion through the increased solubility of  $\text{KHCO}_3$ , and this effect compensates for the loss of efficiency from the increased energy needed for heating.

If solid potassium bicarbonate is formed, a further factor affecting energy efficiency is the heat of crystallization of this salt. However, recovering this heat presents technical challenges which limit possibilities for improving energy efficiency (see Supplemental Information).

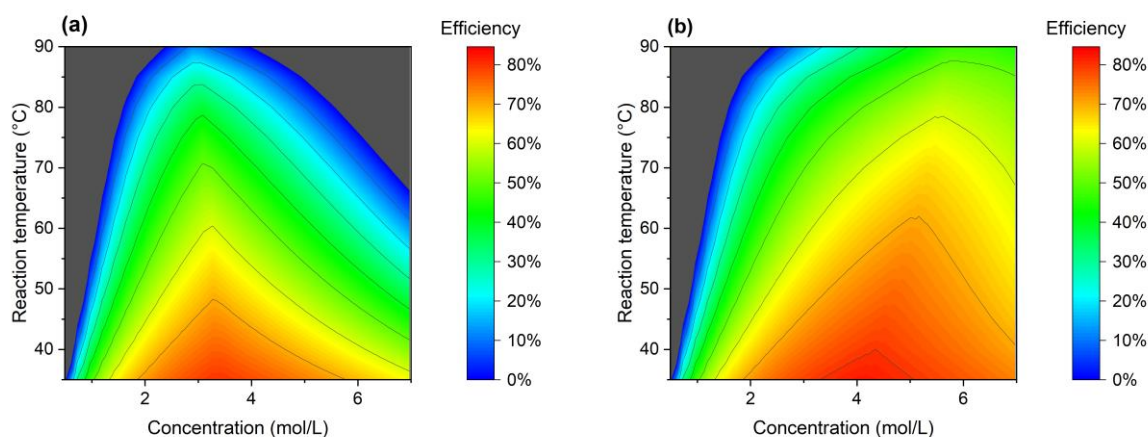


**Figure 6:** Energy efficiency of hydrogen release as a function of temperature and formate concentration under the assumption that the reaction proceeds until either full conversion is achieved or precipitation of bicarbonate starts. The precipitation limit is at 20 °C for (a) and the reaction temperature for (b). Regions where the efficiency is < 0 are shaded in grey.

### 3.4 Storage Density

The addition of water to make formate solutions beyond the equimolar quantity needed stoichiometrically for hydrogen release contributes to both mass and volume, decreasing the

overall energy density. Pure dry potassium formate could release 45 g H<sub>2</sub>/L, although it requires an equimolar quantity of water. A 5 M solution stores 10 g H<sub>2</sub>/L, i.e. less than a quarter of the hydrogen compared to the solid salt. Furthermore, the conversion limits discussed above will also lower the energy density. The calculated volumetric storage densities based on these conversion limits are shown in Figure S7, and selected values are tabulated in Table S1. At a fixed reaction temperature, the efficiencies and storage densities are directly correlated and a concentration with optimal efficiency and density can be identified. For example, at a reaction temperature of 80 °C both properties are highest for 5.5 M potassium formate when precipitation of KHCO<sub>3</sub> occurs only below the reaction temperature. By contrast, efficiency and capacity are inversely correlated with respect to temperature. Low temperatures favor high efficiencies and high temperatures favor high storage density, although the drop in efficiency is not too great when the requirement for complete solubility is limited to the reactor.

### 3.5 Optimal Conditions

When solubility in the reactor is considered as the limit, both the hydrogen storage capacity and energy efficiency show maxima between concentrations of 4.3 M and 5.7 M at 35 °C and 90 °C respectively (Figure S7). The relative value placed on capacity and efficiency will determine which concentration and temperature are optimal; however 5.5 M and 80 °C provides a capacity of 9.1 g H<sub>2</sub>/L and an efficiency of 59 %. The energy inputs are shown in Table 1, compared to those for methylcyclohexane (MCH) which may be considered one of the most mature LOHCs. Both have an energy efficiency of 59%, although have a different balance of energy input. Most of the energy required to release H<sub>2</sub> from MCH comes from the reaction enthalpy, which is not recoverable through heat integration within the dehydrogenation process. By contrast, the largest input for potassium formate is the combination of sensible and latent heats which are amenable to integration.

**Table 1.** Energy inputs (kJ/mol H<sub>2</sub>) for hydrogen release from 5.5 M potassium formate (at 80 °C) and methylcyclohexane. Efficiencies are calculated using 241.9 kJ/mol H<sub>2</sub> for the energy content of hydrogen. Values for methylcyclohexane are for 95% conversion at 320 °C [30].

Property	K formate (5.5 M)	Methylcyclohexane
Sensible heat	49	21
Latent heat	31	11

Reaction enthalpy	20	68
Efficiency	59%	59%

The latent heat of vaporization is the most sensitive to temperature, and this could be partially recovered through heat exchange between the gas exiting the reactor and the incoming liquid. Table 2 shows the amount of heat that can be recovered by cooling the hydrogen stream to various temperatures, and the corresponding efficiency gains. This shows that an energy efficiency of 71% can be achieved if the gas were cooled to 40 °C.

**Table 2.** Possible energy recovery from the gas stream following hydrogen release from 5.5 M potassium formate at 80 °C, cooled to various temperatures. The latent heat comes from condensation of water in the hydrogen stream.

$T_{\text{cool}}$	Latent heat	Sensible heat	Total	Efficiency
(°C)	kJ / (mol H <sub>2</sub> )			
70	12	0.6	13	64%
60	21	1.1	22	68%
50	26	1.7	28	70%
40	29	2.2	31	71%
30	31	2.8	33	72%

The reaction rate is also an important consideration, but is beyond the scope of the present study. However, literature reports [7,31,32] indicate that high conversions (> 80 %) can be obtained relatively quickly using heterogeneous catalysts at ca. 80 °C and 5 M. For example, Hwang et al. [32] show 80 % conversion from 5 M NaHCO<sub>2</sub> after 30 minutes reaction at 80 °C using a 3 wt.% Pd/C catalyst. These results suggest that reactors can be designed to operate under these conditions with a reasonable space-time yield. Further work is underway to investigate the performance of continuous packed-bed reactors for hydrogen release from aqueous formate.

#### 4. Conclusions

The solubility of potassium bicarbonate imposes a practical limit on the concentration of potassium formate solutions used for hydrogen storage, and influences both the hydrogen storage capacity and energy efficiency of hydrogen release. At a fixed temperature, both

capacity and efficiency increase with increasing formate concentration up to the solubility limit of the bicarbonate salt. Beyond this concentration, the common ion effect reduces bicarbonate solubility markedly and decreases the conversion achievable before bicarbonate precipitation. This reduces capacity and efficiency below their values for full conversion of a less concentrated formate solution. The effect is exacerbated by the fact that water is not only a solvent, but also a reactant. As a consequence, the hydrogen release reaction leads to an increase in overall salt concentration, which should be taken into account when considering solubility limits. Higher temperatures increase solubility and therefore hydrogen storage capacity, but also increase the energy required to heat the formate solution to the reaction temperature. This effect is strongest at low formate concentrations and becomes less important above ~3 M. By considering all these effects, as well as thermodynamic equilibria, a concentration of 5.5 M and a reaction temperature of 80 °C were identified as optimum conditions for hydrogen release from potassium formate. These conditions balance heat demand and solubility, leading to an energy efficiency of 59% before heat integration, and a volumetric capacity of 9.1 g H<sub>2</sub>/L. Efficiency can be boosted to 71% by recovering most of the latent heat of vaporization from the gas exiting the reactor, Future work will develop a process engineering model for these conditions and lead to cost estimates for hydrogen storage using aqueous potassium formate.

**Acknowledgments.** This work was supported by the US Department of Energy (DOE), Office of Energy Efficiency and Renewable Energy. The authors gratefully acknowledge research support from the Hydrogen Materials - Advanced Research Consortium (HyMARC), established as part of the Energy Materials Network under the U.S. Department of Energy, Office of Energy Efficiency and Renewable Energy, Hydrogen and Fuel Cell Technologies Office, under Contract Number No. DE-AC36-08GO28308.

## References

1. C. Chu, K. Wu, B. Luo, Q. Cao and H. Zhang, *Hydrogen storage by liquid organic hydrogen carriers: Catalyst, renewable carrier, and technology – A review*. Carbon Resources Conversion, 2023. **6**(4): p. 334–351.
2. P. Preuster, C. Papp and P. Wasserscheid, *Liquid Organic Hydrogen Carriers (LOHCs): Toward a Hydrogen -free Hydrogen Economy*. Accounts of Chemical Research, 2017. **50**(1): p. 74–85.
3. S. Ramadhani, Q.N. Dao, Y. Imanuel, M. Ridwan, H. Sohn, H. Jeong, K. Kim, C.W. Yoon, K.H. Song and Y. Kim, *Advances in Catalytic Hydrogenation of Liquid Organic*

- Hydrogen Carriers (LOHCs) Using High-Purity and Low-Purity Hydrogen*. Chemcatchem, 2024. **16**(24).
4. P.T. Aakko-Saksa, C. Cook, J. Kiviaho and T. Repo, *Liquid organic hydrogen carriers for transportation and storing of renewable energy – Review and discussion*. J. Power Sources, 2018. **396**: p. 803–823.
  5. P.M. Modisha, C.N.M. Ouma, R. Garidzirai, P. Wasserscheid and D. Bessarabov, *The Prospect of Hydrogen Storage Using Liquid Organic Hydrogen Carriers*. Energy Fuels, 2019. **33**(4): p. 2778–2796.
  6. R. Williams, R.S. Crandall and A. Bloom, *Use of Carbon-Dioxide in Energy-Storage*. Applied Physics Letters, 1978. **33**(5): p. 381–383.
  7. H. Wiener, Y. Sasson and J. Blum, *Palladium-Catalyzed Decomposition of Aqueous Alkali-Metal Formate Solutions*. Journal of Molecular Catalysis, 1986. **35**(3): p. 277–284.
  8. Y. Chen, X. Kong, C.S. Yang, Y.H. Liao, G. Gao, R. Ma, M. Peng, W.P. Shao, H. Zheng, H. Zhang, X. Pan, F. Yang, Y.L. Zhu, Z. Liu, Y. Cao, D. Ma, X.H. Bao and Y.F. Zhu, *A catalytic cycle that enables crude hydrogen separation, storage and transportation*. Nature Energy, 2025. **10**(8): p. 971–980.
  9. E. Santacesaria, R. Tesser, S. Fulignati and A.M.R. Galletti, *The Perspective of Using the System Ethanol-Ethyl Acetate in a Liquid Organic Hydrogen Carrier (LOHC) Cycle*. Processes, 2023. **11**(3).
  10. H. Jorschick, P. Preuster, S. Dürr, A. Seidel, K. Müller, A. Bösmann and P. Wasserscheid, *Hydrogen storage using a hot pressure swing reactor*. Energy & Environmental Science, 2017. **10**(7): p. 1652–1659.
  11. R.H. Crabtree, *Nitrogen-Containing Liquid Organic Hydrogen Carriers: Progress and Prospects*. ACS Sustainable Chemistry & Engineering, 2017. **5**(6): p. 4491–4498.
  12. B.S. Shin, C.W. Yoon, S.K. Kwak and J.W. Kang, *Thermodynamic assessment of carbazole-based organic polycyclic compounds for hydrogen storage applications via a computational approach*. International Journal of Hydrogen Energy, 2018. **43**(27): p. 12158–12167.
  13. K. Stark, V.N. Emel'yanenko, A.A. Zhabina, M.A. Varfolomeev, S.P. Verevkin, K. Müller and W. Arlt, *Liquid Organic Hydrogen Carriers: Thermophysical and Thermochemical Studies of Carbazole Partly and Fully Hydrogenated Derivatives*. Industrial & Engineering Chemistry Research, 2015. **54**(32): p. 7953–7966.
  14. K. Müller, K. Brooks and T. Autrey, *Hydrogen Storage in Formic Acid: A Comparison of Process Options*. Energy & Fuels, 2017. **31**(11): p. 12603–12611.
  15. H. Zhong, M. Iguchi, F.Z. Song, M. Chatterjee, T. Ishizaka, I. Nagao, Q. Xu and H. Kawanami, *Automatic high-pressure hydrogen generation from formic acid in the presence of nano-Pd heterogeneous catalysts at mild temperatures*. Sustainable Energy & Fuels, 2017. **1**(5): p. 1049–1055.
  16. K. Müller, J. Völkl and W. Arlt, *Thermodynamic Evaluation of Potential Organic Hydrogen Carriers*. Energy Technology, 2013. **1**(1): p. 20–24.
  17. D.C. Engel, G.F. Versteeg and W.P.M. van Swaaij, *Chemical equilibrium of hydrogen and aqueous solutions of 1:1 bicarbonate and formate salts with a common cation*. Fluid Phase Equilibria, 1997. **135**(1): p. 109–136.
  18. O.Y. Gutiérrez, K. Grubel, J. Kothandaraman, J.A. Lopez-Ruiz, K.P. Brooks, M.E. Bowden and T. Autrey, *Using earth abundant materials for long duration energy storage: electro-chemical and thermo-chemical cycling of bicarbonate/formate*. Green Chemistry, 2023. **25**(11).

19. D. Schubert, D. Neiner, M. Bowden, S. Whitemore, J. Holladay, Z.G. Huang and T. Autrey, *Capacity enhancement of aqueous borohydride fuels for hydrogen storage in liquids*. *Journal of Alloys and Compounds*, 2015. **645**: p. S196–S199.
20. K. Sordakis, A.F. Dalebrook and G. Laurenczy, *A Viable Hydrogen Storage and Release System Based on Cesium Formate and Bicarbonate Salts: Mechanistic Insights into the Hydrogen Release Step*. *Chemcatchem*, 2015. **7**(15): p. 2332–2339.
21. Q.L. Zhang, Y. Wu, X.L. Sun and J. Ortega, *Kinetics of catalytic hydrolysis of stabilized sodium borohydride solutions*. *Industrial & Engineering Chemistry Research*, 2007. **46**(4): p. 1120–1124.
22. A. Bahuguna and Y. Sasson, *Formate-Bicarbonate Cycle as a Vehicle for Hydrogen and Energy Storage*. *Chemsuschem*, 2021. **14**(5): p. 1258–1283.
23. K. Koh, M. Jeon, D.M. Chevrier, P. Zhang, C.W. Yoon and T. Asefa, *Novel nanoporous N-doped carbon-supported ultrasmall Pd nanoparticles: Efficient catalysts for hydrogen storage and release*. *Applied Catalysis B-Environmental*, 2017. **203**: p. 820–828.
24. R. Shirman, A. Bahuguna and Y. Sasson, *Effect of precursor on the hydrogen evolution activity and recyclability of Pd-Supported graphitic carbon nitride*. *International Journal of Hydrogen Energy*, 2021. **46**(73): p. 36210–36220.
25. J. Su, L.S. Yang, M. Lu and H.F. Lin, *Highly Efficient Hydrogen Storage System Based on Ammonium Bicarbonate/Formate Redox Equilibrium over Palladium Nanocatalysts*. *Chemsuschem*, 2015. **8**(5): p. 813–816.
26. K. Grubel, J. Su, J. Kothandaraman, K. Brooks, G.A. Somorjai and T. Autrey, *Research Requirements to Move the Bar forward Using Aqueous Formate Salts as H<sub>2</sub> Carriers for Energy Storage Applications*. *Journal of Energy and Power Technology*, 2020. **02**(04): p. 016.
27. Y. Sasson, H. Wiener and A. Givant, *Method for storage and release of hydrogen*. 2020, YISSUM RES DEV CO OF HEBREW UNIV JERUSALEM LTD: US.
28. T. Wen, M. Wang, Y. Chen, W.F. He and Y.M. Luo, *Thermal properties study and performance investigation of potassium formate solution in a falling film dehumidifier/regenerator*. *International Journal of Heat and Mass Transfer*, 2019. **134**: p. 131–142.
29. H. Wiener, J. Blum, H. Feilchenfeld, Y. Sasson and N. Zalmanov, *The Heterogeneous Catalytic-Hydrogenation of Bicarbonate to Formate in Aqueous-Solutions*. *Journal of Catalysis*, 1988. **110**(1): p. 184–190.
30. Y. Okada, E. Sasaki, E. Watanabe, S. Hyodo and H. Nishijima, *Development of Dehydrogenation Catalyst for Hydrogen Generation in Organic Chemical Hydride Method*. *Int. J. Hydrog. Energy* 2006. **31**(10): p. 1348–1356. <https://doi.org/10.1016/j.ijhydene.2005.11.014>.
31. Q. Bi, J. Lin, Y. Liu, X. Du, J. Wang, H. He, and Y. Cao, *An Aqueous Rechargeable Formate-Based Hydrogen Battery Driven by Heterogeneous Pd Catalysis*. *Angew. Chem. Int. Ed.*, 2014. **53**(49): p. 13583–13587. <https://doi.org/10.1002/anie.201409500>.
32. Y.J Hwang, Y. Kwon, Y. Kim, H. Sohn, S.W. Nam, J. Kim, T. Autrey, C.W. Yoon, Y.S. Jo, and H. Jeong, *Development of an Autothermal Formate-Based Hydrogen Generator: From Optimization of Formate Dehydrogenation Conditions to Thermal Integration with Fuel Cells*. *ACS Sustain. Chem. Eng.*, 2020. **8**(26): p. 9846–9856. <https://doi.org/10.1021/acssuschemeng.0c02775>.